Electronic supplementary information

Judicious selection of a pinhole defect filler to generally enhance the performance of organic dye-sensitized solar cells

Min Zhang, Jing Zhang, Ye Fan, Lin Yang, Yinglin Wang, Renzhi Li and Peng Wang*

State Key Laboratory of Polymer Physics and Chemistry, Changchun Institute of Applied Chemistry, Chinese Academy of Sciences, Changchun 130022, China

Experimental details

Materials. Acetonitrile, *tert*-butanol and chlorobenzene were distilled before use. Pd(OAc)$_2$ and 2-(2',6'-dimethoxybiphenyl)dicyclohexylphosphine (Sphos) were purchased from Sigma-Aldrich and used without further purification.

4,4,5,5-Tetramethyl-2-{4-[*N,N*-bis(9,9-diethyl-7-(hexyloxy)-9*H*-fluoren-2-yl)amino]phenyl}-1,3,2-dioxaborolane,[S1]

5-[6-(5-bromothiophen-2-yl)-4,4-didodecyl-4*H*-cyclopenta[2,1-*b*:3,4-*b*']dithiophen-2-yl]thiophene-2-carbaldehyde,[S2] filler **I**,[S3] filler **II**,[S4] filler **III**,[S5] **C218**,[S1] **C219**,[S6] **C229**,[S2] **C249**[S7] and **C250**[S7] were synthesized according to the literature procedures. The synthetic details of **C256** are described as follows.

5-{6-{5-{4-{Bis[9,9-diethyl-7-(hexyloxy)-9*H*-fluoren-2-yl]amino}phenyl}thiophen-2-yl}-4,4-didodecyl-4*H*-cyclopenta[2,1-*b*:3,4-*b*']dithiophen-2-yl}thiophene-2-carbaldehyde. To a solution of 4,4,5,5-tetramethyl-2-{4-[*N,N*-bis(9,9-diethyl-7-(hexyloxy)-9*H*-fluoren-2-yl)amino]phenyl}-1,3,2-dioxaborolane (0.154 g, 0.18 mmol), 5-[6-(5-bromothiophen-2-yl)-4,4-didodecyl-4*H*-cyclopenta[2,1-*b*:3,4-*b*']dithiophen-2-yl]thiophene-2-carbaldehyde (0.118 g, 0.15 mmol) and K$_3$PO$_4$ (0.160 g, 0.75 mmol) in 1,4-dioxane/H$_2$O (10 mL, 5/1, v/v) were added Pd(OAc)$_2$ (0.002 g, 0.01 mmol) and SPhos (0.004 g, 0.01 mmol). The reaction mixture was stirred at room temperature for 12 h under argon and then water (20 mL) added. The crude product was extracted into ethyl acetate, and the organic layer was washed with brine and water, dried over anhydrous sodium sulfate. After removing solvent under reduced pressure, the residue was purified by column chromatography (ethyl acetate/petroleum ether 60–90 ºC, 1/50, v/v) on silica gel to yield a red solid as the desired product (0.171 g, 79% yield). ^{1}H NMR (400 MHz, THF-d_8) δ: 9.82 (s, 1H), 7.75 (d, J = 4.0 Hz, 1H), 7.55 (m, 6H), 7.45 (s, 1H), 7.34 (d, J = 4.0 Hz, 1H), 7.22 (m, 9H), 6.89 (m, 4H), 4.01 (t, J = 6.4 Hz, 4H), 1.93 (m, 12H), 1.80 (m, 4H), 1.53 (m, 4H), 1.38 (m, 8H), 1.26 (m, 36H), 1.04 (m, 4H), 0.94 (m, 6H), 0.87 (t, J = 6.6 Hz, 6H), 0.36 (t, J = 7.2 Hz, 12H). ^{13}C NMR (100 MHz, THF-d_8) δ: 182.71, 161.36, 160.59, 160.25, 152.76, 152.01, 149.49, 148.61, 147.34, 144.34, 142.73, 140.99, 139.88, 138.88, 138.60, 137.58, 137.44, 135.93, 135.53, 128.77, 127.36, 125.48, 125.02, 124.37, 124.16, 121.95, 121.07, 120.78, 120.67, 119.17, 114.24, 110.58, 69.19, 57.40, 55.72, 39.07, 34.07, 33.31, 33.12, 31.42, 31.04, 30.89, 30.74, 27.27, 25.88, 14.97, 14.93, 9.49. MS (ESI) *m/z* calcd. for (C$_{94}$H$_{119}$NO$_3$S$_4$): 1437.81. Found: 1438.78 ([M+H]$^+$). Anal. calcd. for C$_{94}$H$_{119}$NO$_3$S$_4$: C, 78.45; H, 8.33; N, 0.97. Found: C, 78.27; H, 8.39; N, 1.02.

3-{5-{6-{5-{4-{Bis[9,9-diethyl-7-(hexyloxy)-9*H*-fluoren-2-yl]amino}phenyl}thiophen-2-yl}-4,4-didodecyl-4*H*-cyclopenta[2,1-*b*:3,4-*b*']dithiophen-2-yl}thiophene-2-yl}-2-cyanoacrylic acid (C256). To a stirred solution of 5-{6-{5-{4-{Bis[9,9-diethyl-7-(hexyloxy)-9*H*-fluoren-2-yl]amino}phenyl}thiophen-2-yl}-4,4-didodecyl-4*H*-cyclopenta[2,1-*b*:3,4-*b*']dithiophen-2-yl}thiophene-2-carbaldehyde (0.120 g, 0.083 mmol) and cyanoacetic acid (0.021 g, 0.25 mmol) in chloroform (15 mL) was added piperidine (0.055 mL, 0.55 mmol). The resulting mixture was refluxed for 12 h and then cooled to room temperature before acidified with 2 M hydrochloric acid aqueous solution. The solution was extracted into chloroform, and the organic phase was washed with water, and dried over anhydrous sodium sulfate. After removing solvent under reduced pressure, the crude product was purified by column chromatography (methanol/chloroform, 1/30, v/v) over silica gel to afford a black powder as the desired product (0.092 g, 73% yield). ^{1}H NMR (400 MHz, THF-d_8) δ: 8.32 (s, 1H), 7.76 (d, J = 4.0 Hz, 1H), 7.55 (m, 7H), 7.35 (d, J = 4.0 Hz, 1H), 7.23 (m, 3H), 7.11 (m, 6H), 6.86 (m, 4H), 4.01 (t, J = 6.4 Hz, 4H), 1.93 (m, 12H), 1.70 (m, 4H), 1.38 (m, 4H), 1.29 (m, 8H), 1.26 (m, 36H), 1.03 (m, 4H), 0.93 (m, 6H), 0.86 (t, J = 7.0 Hz, 6H), 0.35 (t, J = 7.2 Hz, 12H). ^{13}C NMR (100 MHz, THF-d_8) δ: 164.67, 161.66, 160.63, 152.77, 152.02, 149.53, 149.18, 147.36, 146.72, 144.42, 141.24, 141.10, 140.41, 138.92, 137.44, 135.99, 135.56, 135.24, 128.78, 127.36, 125.55, 125.03, 124.42, 124.25, 124.16, 122.36, 121.06, 120.76, 120.68, 119.21, 117.28, 114.26, 110.55, 99.21, 69.20, 57.42, 55.85, 39.13, 34.07, 33.32, 33.13, 31.41, 31.05, 30.90, 30.75, 27.27, 24.01, 14.91, 14.87, 14.86, 9.43. HR-MS (MALDI) *m/z* calcd. for (C$_{97}$H$_{120}$N$_2$O$_4$S$_4$): 1504.81309.

Found: 1504.81237. Anal. calcd. for $C_{97}H_{120}N_2O_4S_4$: C, 77.35; H, 8.03; N, 1.86. Found: C, 77.16; H, 8.17; N, 1.92. ATR-FTIR σ_{max}: 1687 cm^{-1} (COOH), 2218 cm^{-1} (CN).

UV-vis, ATR-FITR and voltammetric measurements. UV-vis spectra were recorded on an Agilent G1103A spectrometer equipped with a silicon diode array detector. ATR-FTIR spectra were obtained with a BRUKER Vertex 70 FTIR spectrometer. Square-wave voltammograms of the THF dye solutions were measured on a CHI660C electrochemical workstation, using a mini-electrolytic cell composed of a platinum ultramicroelectrode, a platinum gauze counter electrode and a silver-wire auxiliary electrode. The potential was reported against the Fc/Fc$^+$ reference.

Cell fabrication and characterization. A 4.3+5.0-μm-thick, double-layer titania film made *via* screen-printing on a pre-cleaned fluorine-doped tin oxide (FTO) conducting glass (Nippon Sheet Glass, Solar, 4 mm thick) was deployed as the negative electrode of DSCs presented in this paper. A translucent layer of 25-nm-sized titania particles was first deposited on a FTO glass and further covered with a light-scattering layer of 350–450-nm-sized titania particles (WER4-O, Dyesol). Preparation procedures for titania nanocrystals, screen-printing pastes and nanostructured titania films were very similar to those described in a previous paper.[S8] The detailed dyeing processes for these cells were listed in Table S2. The dye-grafted titania electrode was assembled with a thermally platinized FTO electrode by use of a 25-μm-thick Surlyn ring to produce a thin-layer electrochemical cell. Two analogous cobalt electrolytes (Co-phen and Co-bpy) were used here to match the ground-state oxidation potentials of dye molecules. Notice that the redox potential of Co-phen is about 70 mV more positive than that of Co-bpy. The Co-phen electrolyte is composed of 0.25 M tris(1,10-phenanthroline)cobalt(II) di[bis(trifluoromethanesulfonyl)imide], 0.05 M tris(1,10-phenanthroline)cobalt(III) tris[bis(trifluoromethanesulfonyl)imide], 0.5 M 4-*tert*-butylpyridine and 0.1 M lithium bis(trifluoromethanesulfonyl)imide in acetonitrile. Replacement of tris(1,10-phenanthroline)cobalt in Co-phen with tris(2,2′-bipyridine)cobalt affords the Co-bpy counterpart. Details on IPCE, *j–V* and photovoltage decay measurements can be found in our previous publication.[S9]

Femtosecond fluorescence up-conversion measurements. A mode-locked Ti:sapphire laser (Tsunami, Spectra Physics) pumped by a Nd:YVO$_4$ laser (Millennia Pro s-Series, Spectra Physics) was employed to seed a regenerative amplifier (RGA, Spitfire, Spectra Physics). The output of 3.7 mJ femtosecond pulse (130 fs pulse width) at 800 nm from the amplifier was divided into two parts with a 9/1 beam splitter. The large proportion was sent to an optical parametric amplifier (TOPAS-C, Light Conversion) to generate the pump pulse (480 nm), and the pump laser pulse fluence is fixed at 22 μJ cm^{-2}. Both the 720 nm photons emitted from the rotating sample and the minor part of the RGA output serving as the optical gate were focused onto a 0.3-mm-thick BBO crystal to generate a sum frequency light in a femtosecond fluorescence up-conversion spectrometer (FOG 100-DA, CDP Corp.). The FWHM of our instrument response function was approximately 180 fs.

X-Ray photoelectron spectroscopy (XPS) and X-ray reflectivity (XRR) measurements. XPS spectra were recorded with an ESCALAB 250 spectrometer equipped with a hemispherical electron energy analyzer using the Al Kα radiation (hv = 1486.6 eV) and an energy step of 0.1 eV. The electron take-off angle (α) was 90°. Photoelectron spectra were measured in constant analyzer energy (CAE) mode. The spectra are energy calibrated by setting the Ti2p$_{3/2}$ signal to 458.6 eV.[S10] If a compact dye layer is simply assumed to locate on the surface of titania, the Ti2p$_{3/2}$ signal intensity can be quantitatively related with the mean thickness of a compressed dye layer (d_p), *via* a two-layer model $I = I_0 \exp(-d/\lambda\sin\alpha)$,[S11] where I_0 is the signal intensity of a bare titania substrate, α is 90° and λ the inelastic electron mean free path (IMFP) in a compact organic solid composed of dye molecules. The λ values of fillers **I**, **II** and **III**, being 30.9, 30.8 and 31.8 Å, respectively, were computed with the aid of some semi-empirical equations and parameters in the literature,[S12] and the d values of filler coating on titania were further derived as 11.2 Å for filler **I**, 32.6 Å for filler **II** and 37.2 Å for filler **III**, in terms of the Ti2p$_{3/2}$ intensities. XRR measurements were carried out on a Bruker D8 discover reflectometer using the Cu Kα X-ray radiation (λ = 1.542 Å). The X-ray beam was collimated using a Göbel mirror with a 0.2 mm slit and a postsample parallel collimator. Reflectivity spectra were recorded

over the angular range $0.10° \leq \theta \leq 4.00°$, with a step size of $0.0025°$ and a counting time of 1 s per step. Collected reflectivity data were plotted as a function of perpendicular momentum transfer (Q_Z), $Q_Z = 4\pi(\sin\theta)/\lambda$, and were refined by the MOTOFIT package[S13] to obtain structural parameters associated with layers for the bare and filler-grafted titania films prepared by atomic layer deposition (ALD). Initial structural models were prepared using estimated values of the X-ray scattering length density (SLD) of 31.2×10^{-6} Å^{-2} for the ALD titania films and 10.0×10^{-6} Å^{-2} for the filler layers. A native silicon oxide layer was not considered in the structural models, as little contrast was present between the SLD of the Si wafer (20.1×10^{-6} Å^{-2}) and that of the native oxide (18.9×10^{-6} Å^{-2}). In the structural model, the thickness, SLD, and interfacial roughness of each layer were first estimated by the genetic optimisation method and further refined by the Levenberg–Marquardt method until minimal χ^2 values were obtained. The SLD of reflective layer is given by the relation $SLD = (r_e N_A \rho Z)/M_R$, where r_e is the Compton radius (2.818×10^{-5} Å), N_A is the Avogadro's number, ρ is the mass density of each layer, Z is the sum of the atomic numbers (*i.e.* total number of electrons) for the molecules in each layer, and M_R is the relative molecular mass for the molecules in each layer. Therefore, the mass density of each layer can be extracted from the refinement of SLD and filler molecular formula.

Additional data and analysis

**Table S1** Photophysical and electrochemical data of dyes studied in this paper

Dye	λ_{max}^{abs} ^{a} [nm]	ε_{max}^{abs} ^{a} [10^3 M^{-1} cm^{-1}]	E_{D/D^+} ^{b} [V]
C218	520	55.2	0.200
C256	543	66.0	0.190
C229	542	59.0	0.177
C219	553	54.0	0.110
C249	556	65.0	0.110
C250	563	63.0	0.090

^{a} The wavelength (λ_{max}^{abs}) and molar absorption coefficient (ε_{max}^{abs}) of maximum absorption are derived from the static electronic absorption spectra in THF. ^{b} The ground-state oxidation potentials (E_{D/D^+}) were measured in THF and reported with respect to the standard Fc/Fc$^+$ redox couple.

Table S2 Detailed dyeing conditions and electrolytes for all cells presented in this work

Cell	Dyeing protocol	Electrolyte
1	A titania film was dye-loaded by immersing it into a dye solution of 150 μM **C218** in the solvent mixture of acetonitrile and *tert*-butanol (v/v, 1/1) for 12 h.	Co-phen
2	A titania film was dye-loaded by immersing it into a saturated dye solution of **C256** in the solvent mixture of acetonitrile and *tert*-butanol for 48 h.	Co-phen
3	A titania film was dye-loaded by immersing it into a saturated dye solution of **C256** in the solvent mixture of acetonitrile and *tert*-butanol for 48 h.	Co-bpy
4	A titania film was dye-loaded by immersing it into a dye solution of 100 μM **C256** in chlorobenzene for 12 h.	Co-phen
5	A titania film was dye-loaded by immersing it into a dye solution of 100 μM **C256** in chlorobenzene for 12 h, and was then transferred to pure acetonitrile for 5 min for a parallel test.	Co-phen
6	A titania film was dye-loaded by immersing it into a dye solution of 100 μM **C256** in chlorobenzene for 12 h, and was then transferred to a solution of 1 mM filler **I** in acetonitrile for 5 min for pinhole defect filling.	Co-phen
7	A titania film was dye-loaded by immersing it into a dye solution of 100 μM **C256** in chlorobenzene for 12 h, and was then transferred to a solution of 1 mM filler **II** in acetonitrile for 5 min for pinhole defect filling.	Co-phen
8	A titania film was dye-loaded by immersing it into a dye solution of 100 μM **C256** in chlorobenzene for 12 h, and was then transferred to a solution of 1 mM filler **III** in acetonitrile for 5 min for pinhole defect filling.	Co-phen
9	A titania film was organic-loaded by immersing it into a solution of 100 μM filler **III** in acetonitrile for 12 h.	Co-phen
10	A titania film was organic-loaded by immersing it into a solution of saturated **C256** and 100 μM filler **III** in the solvent mixture of acetonitrile and *tert*-butanol for 48 h.	Co-phen
11	A titania film was dye-loaded by immersing it into a dye solution of 100 μM **C229** in chlorobenzene for 12 h.	Co-phen
12	A titania film was dye-loaded by immersing it into a dye solution of 100 μM **C229** in chlorobenzene for 12 h, and was then transferred to a solution of 1 mM filler **III** in acetonitrile for 5 min for pinhole defect filling.	Co-phen
13	A titania film was dye-loaded by immersing it into a dye solution of 100 μM **C219** in chlorobenzene for 12 h.	Co-bpy[a]
14	A titania film was dye-loaded by immersing it into a dye solution of 100 μM **C219** in chlorobenzene for 12 h, and was then transferred to a solution of 1 mM filler **III** in acetonitrile for 5 min for pinhole defect filling.	Co-bpy[a]
15	A titania film was dye-loaded by immersing it into a dye solution of 100 μM **C249** in chlorobenzene for 12 h.	Co-bpy[a]
16	A titania film was dye-loaded by immersing it into a dye solution of 100 μM **C249** in chlorobenzene for 12 h, and was then transferred to a solution of 1 mM filler **III** in acetonitrile for 5 min for pinhole defect filling.	Co-bpy[a]
17	A titania film was dye-loaded by immersing it into a dye solution of 100 μM **C250** in chlorobenzene for 12 h.	Co-bpy[a]
18	A titania film was dye-loaded by immersing it into a dye solution of 100 μM **C250** in chlorobenzene for 12 h, and was then transferred to a solution of 1 mM filler **III** in acetonitrile for 5 min for pinhole defect filling.	Co-bpy[a]

[a]The relatively negative oxidation potentials of **C219**, **C249** and **C250** limit the use of the Co-phen electrolyte by influencing the hole-injection yield, thus a Co-bpy electrolyte is used.
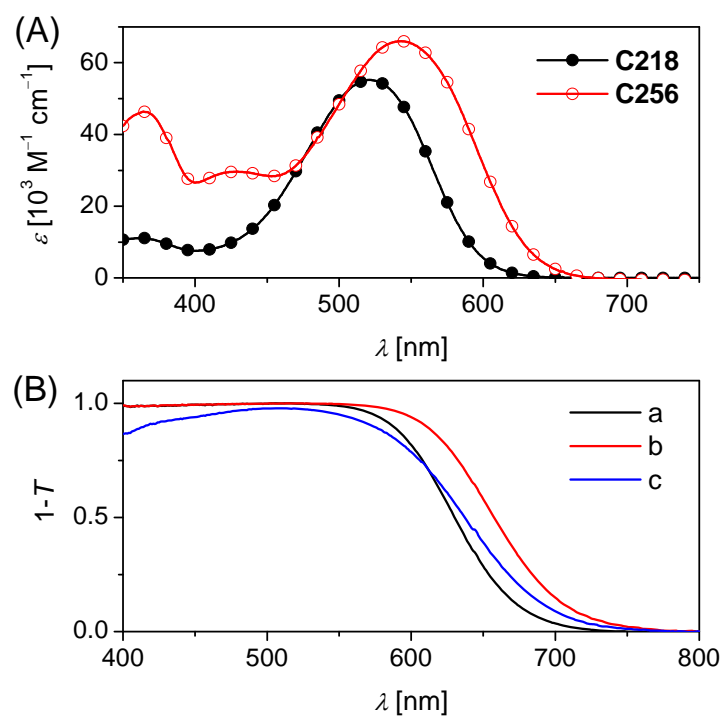
Fig. S1 (A) UV-vis absorption spectra of **C218** and **C256** in THF. (B) Absorption spectra of 4.3-μm-thick, transparent titania films stained *via* the corresponding dyeing protocols for cells 1 (a), 2 (b) and 4 (c).
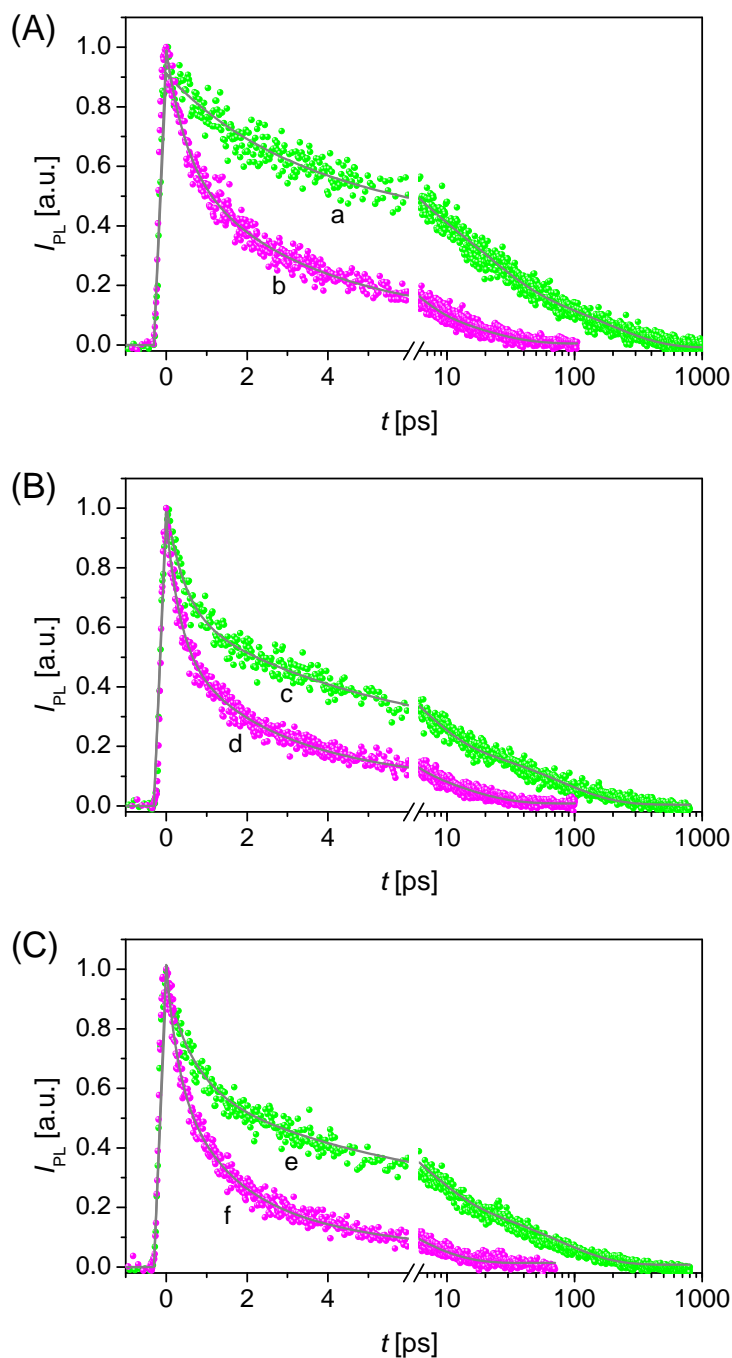
Fig. S2 Femtosecond PL decay traces of alumina films (green dots a, c and e) and titania films (magenta dots b, d and f) dyed with (A) **C218** and (B) **C256** from the solvent mixture of acetonitrile and *tert*-butanol (v/v, 1/1) as well as (C) **C256** from chlorobenzene in combination with the Co-phen electrolyte. Pump wavelength: 480 nm; probe wavelength: 720 nm. The solid gray lines are fittings of normalized PL traces *via* the three-exponential decay equation of $I_{PL} = A_0 + A_1\exp(-t/\tau_1) + A_2\exp(-t/\tau_2) + A_3\exp(-t/\tau_3)$, where A_i and τ_i denote the fractional amplitudes and lifetimes, and $\sum_{i=1}^{n} A_i = 1$.

The femtosecond fluorescence up-conversion technique was resorted to investigate the excited state dynamics of the dye-grafted titania film infiltrated with the Co-phen electrolyte, with the corresponding dye-grafted alumina film as a reference. As shown in Fig. S2, the PL decays for all samples feature multi-exponential, and the corresponding time

coefficients can be obtained by analyzing the data based upon a parallel kinetic model.[S14] The amplitude-averaged lifetimes $<\tau>_{alumina}$ of the **C218**-grafted alumina film are determined to be 50.93 ps, and those of the **C256**-grafted alumina films display obviously shortened values of 18.68 (with the mixture of acetonitrile and *tert*-butanol (v/v, 1/1) as the dye-bath solvent) and 20.21 ps (with chlorobenzene as the dye-bath solvent). The slightly longer $<\tau>_{alumina}$ for **C256** induced by the switch of dye-bath solvent from the mixture of acetonitrile and *tert*-butanol to chlorobenzene could be ascribed to the attenuation of dye aggregation on titania. On the other hand, the amplitude-averaged lifetimes $<\tau>_{titania}$ of dye-grafted titania films are significantly shorter, being 4.00, 3.00 and 1.90 ps for **C218** from the mixture of acetonitrile and *tert*-butanol, **C256** from the mixture of acetonitrile and *tert*-butanol, and **C256** from chlorobenzene, respectively. Furthermore, the electron injection yeilds (ϕ_{ei}) at the titania/dye interface can be roughly estimated according to the equation $\phi_{ei} = 1 - <\tau>_{titania} / <\tau>_{alumina}$. As listed in Table S3, the titania cell with **C256** from the mixture of acetonitrile and *tert*-butanol features a relatively lower ϕ_{ei} of 84% in comparison with the other two cells (92% for **C218** from the mixture of acetonitrile and *tert*-butanol; 91% for **C256** from chlorobenzene), giving a clue on the IPCE summit variation.

Table S3 Time coefficients and relative amplitudes of PL decay traces in Fig. S2

Curve	τ_1 [ps]	A_1	τ_2 [ps]	A_2	τ_3 [ps]	A_3	$\tau_{av}{}^a$ [ps]	ϕ_{ei} [%]
a	2.82	0.39	187.03	0.23	19.57	0.38	50.93	
b	16.53	0.15	2.88	0.48	0.48	0.37	4.00	92
c	5.14	0.44	77.01	0.21	0.45	0.35	18.68	
d	0.34	0.44	11.84	0.17	2.20	0.39	3.00	84
e	0.68	0.35	5.90	0.42	74.83	0.23	20.21	
f	0.27	0.33	5.42	0.24	1.23	0.43	1.90	91

[a] The values of τ_{av} were determined with $<\tau>_{av} = A_1\tau_1 + A_2\tau_2 + A_3\tau_3$.
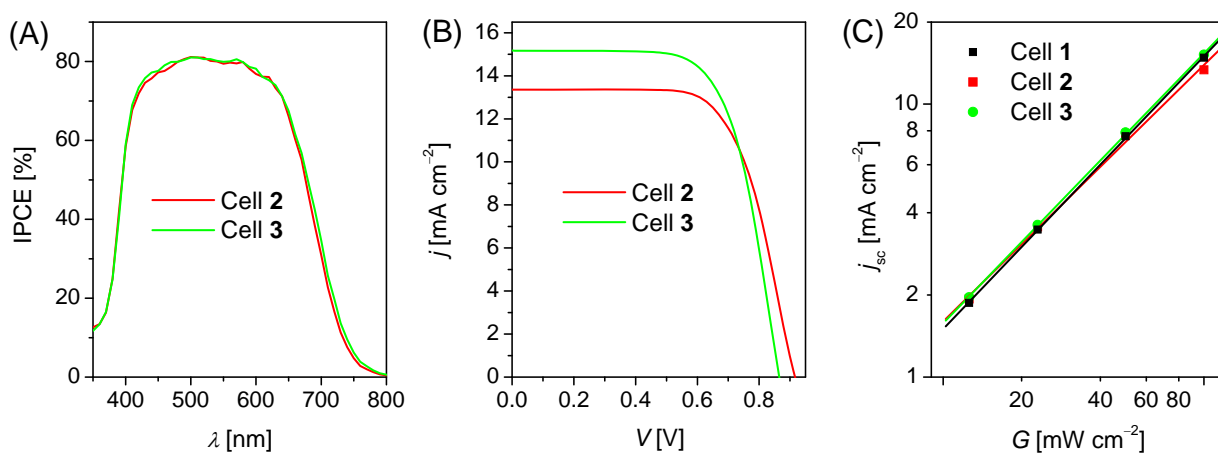
Fig. S3 (A) Photocurrent action spectra of cells 2 and 3. (B) j-V characteristics of cells 2 and 3 measured under an irradiance of 100 mW cm^{-2}, simulated AM 1.5 sunlight. (C) Short-circuit photocurrent density (j_{sc}) plotted as a function of irradiance (G). The experimental data are fitted to a power function $j_{sc} \propto (P_{in})^{\alpha}$, affording the α values of 0.99964 for cell 1, 0.93963 for cell 2 and 0.98924 for cell 3. An antireflection film was adhered to a testing cell during measurement. All cells were tested with a metal shadow mask having an aperture area of 0.160 cm^2.

Table S4 Detailed photovoltaic parameters of all cells measured under an irradiance of 100 mW cm^{-2}, simulated AM1.5 sunlight[a]

Cell	V_{oc} [mV]	j_{sc} [mA cm^{-2}]	FF	η [%]
1	889 (±2)	14.81 (±0.03)	0.716 (±0.003)	9.4 (±0.1)
2	920 (±3)	13.36 (±0.03)	0.664 (±0.004)	8.2 (±0.1)
3	868 (±2)	15.18 (±0.03)	0.672 (±0.005)	8.9 (±0.1)
4	822 (±2)	15.46 (±0.03)	0.747 (±0.003)	9.5 (±0.1)
5	823 (±3)	15.48 (±0.04)	0.752 (±0.004)	9.6 (±0.1)
6	828 (±2)	15.03 (±0.04)	0.751 (±0.003)	9.3 (±0.1)
7	866 (±2)	15.56 (±0.04)	0.730 (±0.002)	9.8 (±0.1)
8	904 (±2)	15.74 (±0.03)	0.737 (±0.002)	10.5 (±0.1)
9	1001 (±2)	9.94 (±0.04)	0.766 (±0.004)	7.6 (±0.1)
10	888(±3)	15.05(±0.03)	0.710(±0.003)	9.5(±0.1)
11	811 (±2)	15.93 (±0.05)	0.746 (±0.004)	9.6 (±0.1)
12	867 (±3)	16.11 (±0.03)	0.723 (±0.003)	10.1 (±0.1)
13	737 (±3)	14.84 (±0.04)	0.752 (±0.004)	8.2 (±0.1)
14	812 (±2)	16.38 (±0.03)	0.708 (±0.003)	9.4 (±0.1)
15	719 (±2)	14.05 (±0.04)	0.743 (±0.004)	7.5 (±0.1)
16	815 (±2)	16.88 (±0.04)	0.712 (±0.004)	9.8 (±0.1)
17	728 (±2)	15.39 (±0.03)	0.751 (±0.003)	8.4 (±0.1)
18	818 (±3)	17.35 (±0.03)	0.717 (±0.004)	10.2 (±0.1)

[a] The deviations of photovoltaic parameters for each kind of cells are listed in brackets based upon five cells. The cell fabrication details can be found from Table S2. An antireflection film was adhered to a testing cell during measurement. All cells were tested with a metal shadow mask having an aperture area of 0.160 cm^2.
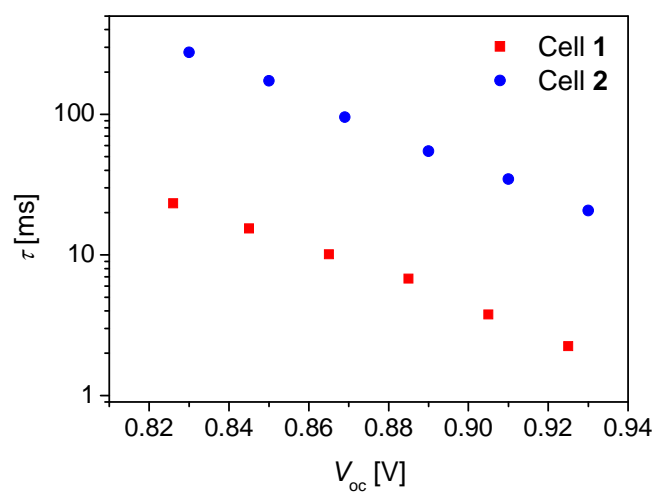
Fig. S4 Electron lifetime (τ) plotted as a function of open-circuit photovoltage (V_{oc}) for cells 1 and 2.
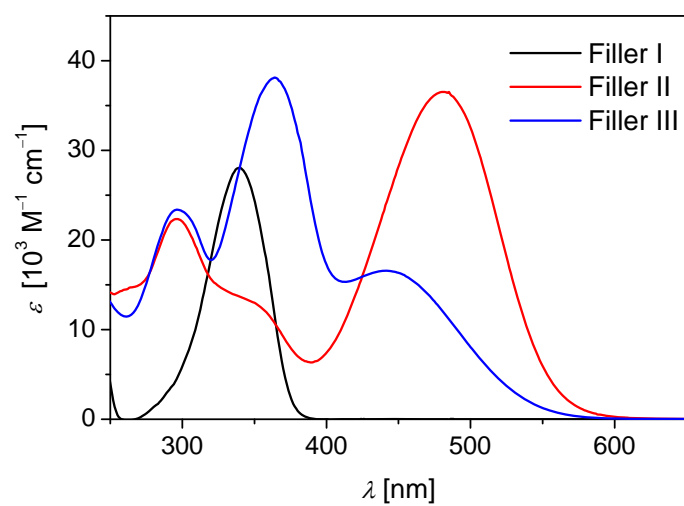
Fig. S5 UV-vis absorption spectra of fillers **I**, **II** and **III** in THF.

Table S5 Refined structural data of molecules adsorbed on the amorphous ALD titania film as well as the mean coating thicknesses and dye loading amount on the mesoporous titania

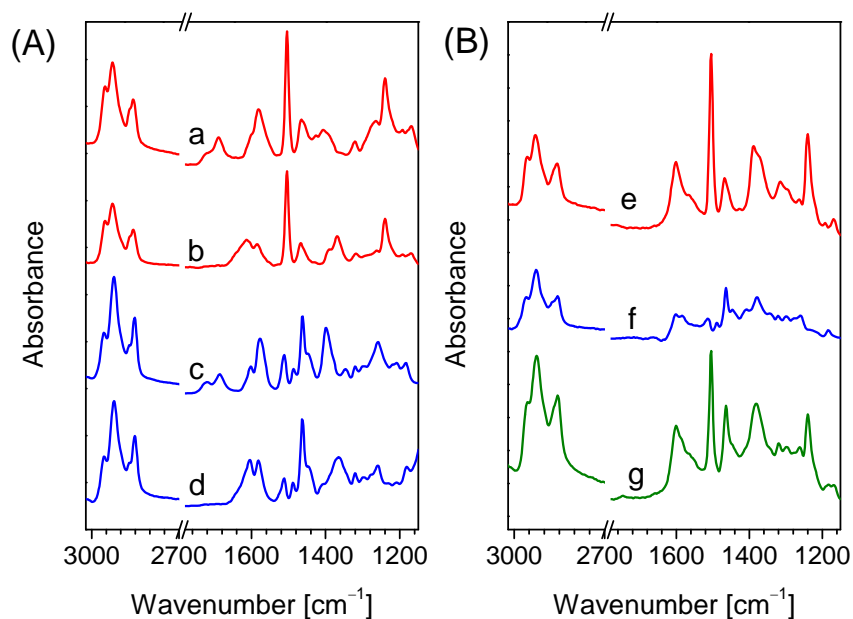|	Bare	Filler **I**	Filler **II**	Filler **III**
Molecular formula	H_2O	$C_{21}H_{31}NO_3$	$C_{38}H_{42}N_2O_4S$	$C_{54}H_{68}N_2O_4S_2$
Molecular layer thickness [Å]	13.1	10.3	15.4	18.7
Molecular layer SLD [$\times 10^{-6}$ Å^{-2}]	9.8	19.2	13.9	12.4
Titania layer thickness [Å]	135.5	134.1	134.7	136.8
Titania layer SLD [$\times 10^{-6}$ Å^{-2}]	31.5	34.2	34.9	35.2
Mass density of molecule [g cm^{-3}]	1.0	2.0	1.5	1.4
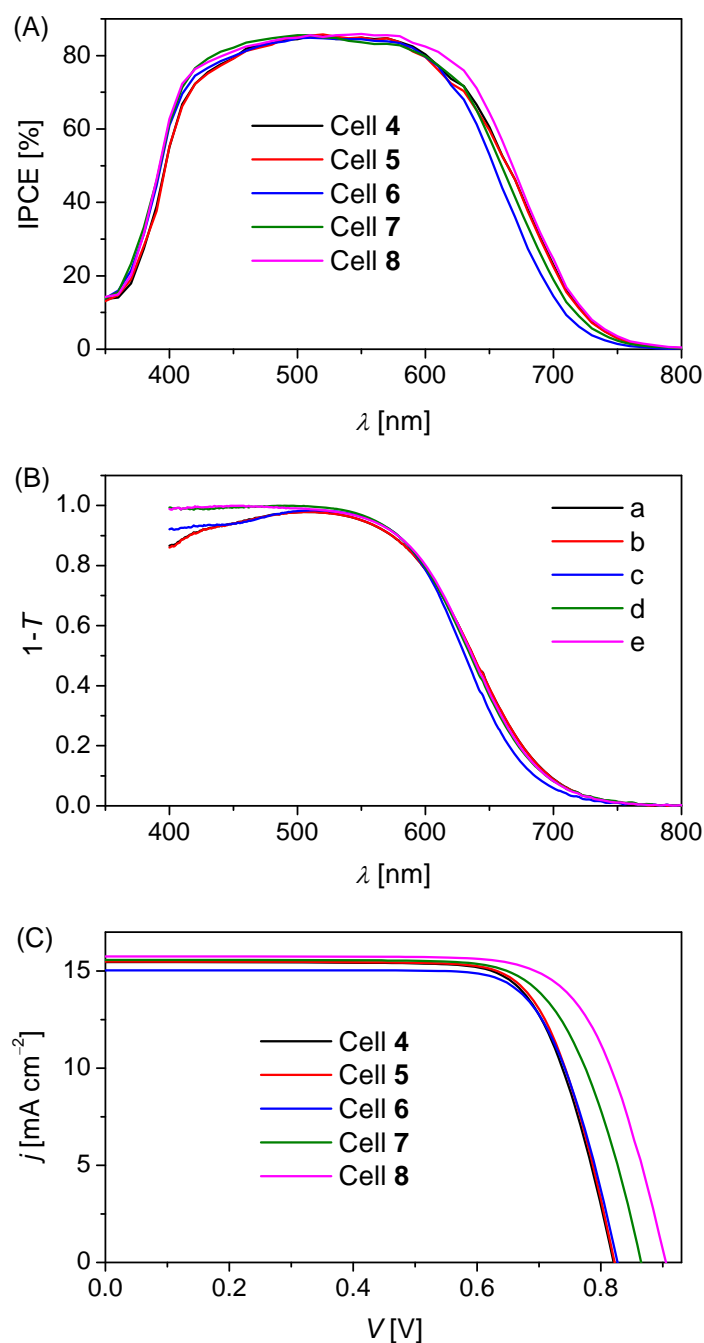
Fig. S6 (A) Photocurrent action spectra of cells 4, 5, 6, 7 and 8. (B) Absorption spectra of 4.3-μm-thick, transparent titania films grafted *via* the corresponding protocols for cells 4 (a), 5 (b), 6 (c), 7 (d) and 8 (e). (C) *j–V* characteristics of cells 4, 5, 6, 7 and 8 measured under an irradiance of 100 mW cm^{-2}, simulated AM 1.5 sunlight. An antireflection film was adhered to a testing cell. The aperture area of our metal mask is 0.160 cm^2. Fillers **I**, **II** and **III** with acetonitrile as the bath solvent were employed to fill the pinhole defects of the titania films grafted with **C256** from chlorobenzene, and the corresponding DSCs were coded as cells 6, 7 and 8, respectively.

As presented in Fig. S6A, cells 5, 6, 7 and 8 display a comparable IPCE summit as cell 4 made with **C256** alone from chlorobenzene. However, cells 6 and 7 display a little bit lower IPCEs in the low energy spectral region compared to cell 4, implying that a small amount of **C256** has been removed from the titania surface during the pinhole defect filling process, albeit the **C256** dye has a very low solubility in actonitrile and the filling time is only 5 min. This deduction was further proved by measuring the electron absorption spectra of the corresponding cells made with transparent titania films (Fig. S6B). Howover, it is worthwhile to note that no difference in either electron absorption or photovoltaic characteristics was probed for

15

the **C256**-grafted titania film immersed in pure acetonitrile for 5 min (cell 5). These observations suggest that even in the poor solvent of acetonitrile, the metathesis of **C256** with fillers **I**, **II** and **III** could occur to some extent. Furthermore, pinhole defect fillers **II** and **III** can enhance the capacity of blue photon capturing (Fig. S5). Moreover, cell 8 has higher IPCEs in the shoulder regions compared to cell 4, suggesting that filler **III** should evoke a higher electron collection efficiency. The *j–V* characteristics (Fig. S6C) of these cells were furhter evaluated under an irradiance of 100 mW cm^{-2}, simulated AM1.5 sunlight, and the detailed parameters were compiled in Table S4. With respect to cell 4 made with **C256** alone from chlorobenzene, cell 7 or 8 with filler **II** or **III** displays an obviously improvement of V_{oc} (44 mV for filler **II**; 82 mV for filler **III**) concomitant with a slightly increased j_{sc}, resulting in an η improvement from 9.5% to 9.8% or to 10.5%, respectively. It is noted that cell 6 with filler **I** does not presents an improved V_{oc} but a decreased j_{sc}, the latter of which results from a slightly reduced light absorption, leading to a decreased η of 9.3%. The V_{oc} enhancement ability of fillers **II** and **III** could be well understood by looking at the relative dark current at a certain potential bias (Fig. 3B of the main text).

Fig. S7 (A) ATR-FTIR spectra of filler **III** (a) and **C256** (c) as well as their sodium salts of filler **III-**Na (b) and **C256**Na (d) spun-cast on the flat quartz. (B) ATR-FTIR spectra of the mesoporous titania films grafted with filler **III** from acetonitrile (e) and **C256** from chlorobenzene (f), as well as sequentially co-grafted with **C256** from chlorobenzene and filler **III** from acetonitrile (g). For clarity of presentation, curves a, b, c, e and f have been vertically displaced and the spectrum of a titania reference film has been subtracted for curves e, f and g.

Compared to the pristine organics spun-cast on the flat quartz, which feature the characteristic carbonyl absorption bands (1689 cm^{-1} for filler **III**; 1685 cm^{-1} for **C256**), both their deprotonated sodium salts and grafted titania films clearly show two new absorption bands (1614 and 1369 cm^{-1} for filler **III-**Na; 1604 and 1365 cm^{-1} for **C256**Na; 1601 and 1388 cm^{-1} for filler **III**/titania; 1600 and 1378 cm^{-1} for **C256**/titania), which can be assigned to the carboxylate asymmetric and symmetric stretching vibrations.[S15] Moreover, the titania film sequentially co-grafted with **C256** and filler **III** also presents the absorption bands for the asymmetric and symmetric stretching of –COO^{-} (1601 and 1381 cm^{-1}). The carbonyl absorption bands cannot be observed for all grafted titania films, ruling out the possibility of weak adsorption of organic molecules on the surface of titania. Moreover, the carboxylate signals of the titania film grafted with **C256** from chlorobenzene alone are relatively weak owing to a lower dye loading amount, but are significantly enhanced after pinhole defect filling with filler **III**. This suggests that a considerable amount of filler **III** has been grafted onto the surface of titania during the pinhole defect filling process.
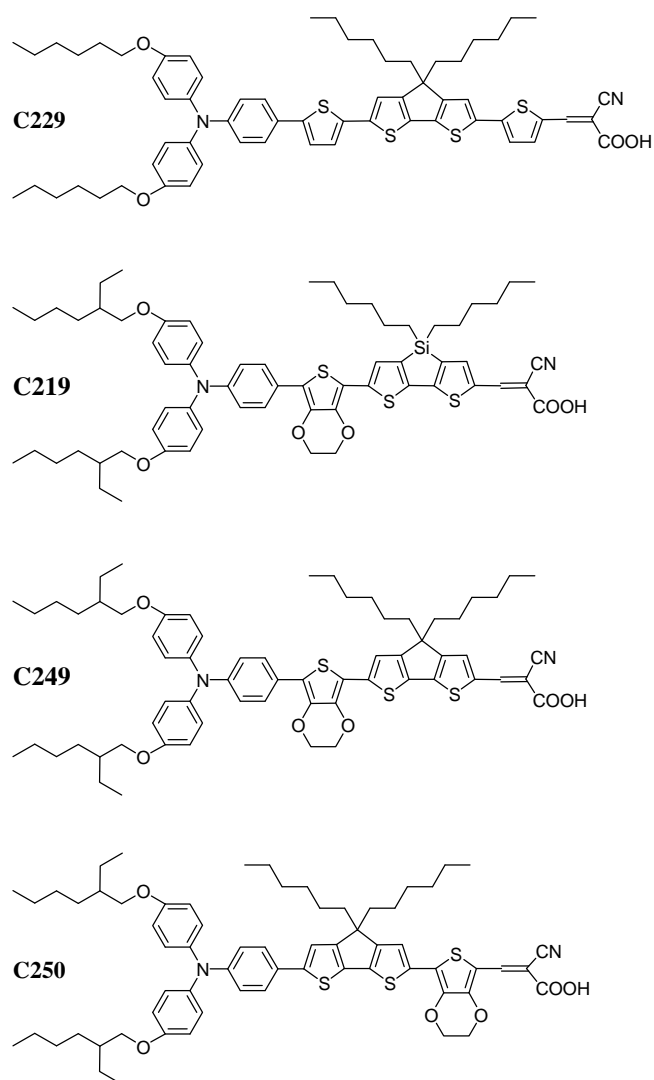
Fig. S8 Molecular structures of **C229**, **C219**, **C249** and **C250** featuring a energy-gap of about 1.55−1.60 eV.
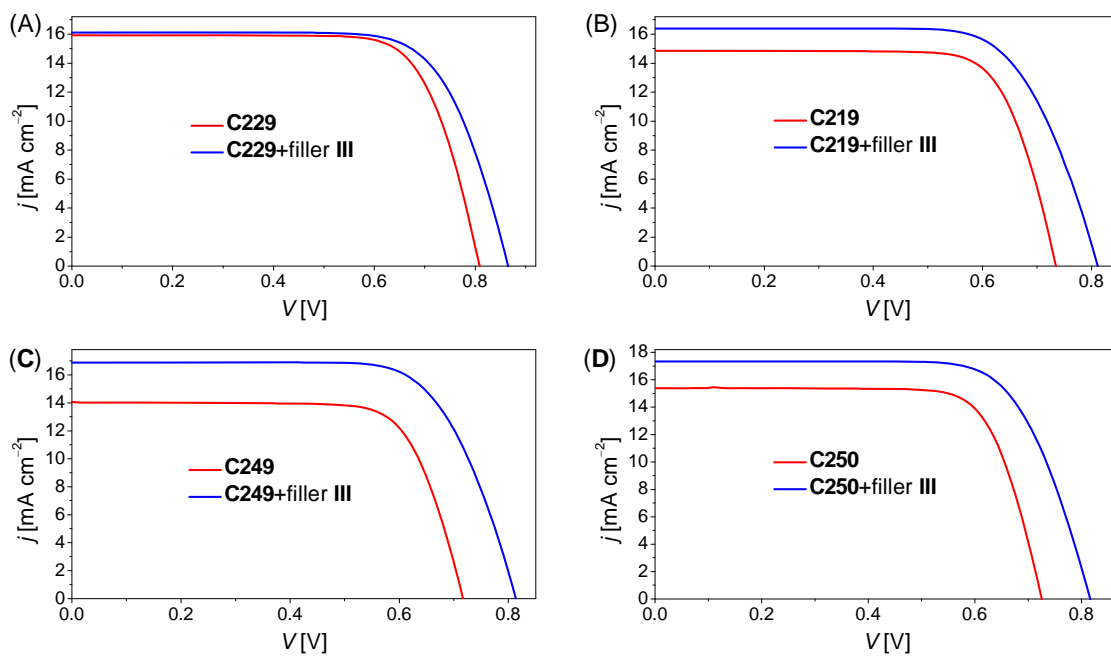
Fig. S9 *j-V* characteristics of cells fabricated by dye-coating with (A) **C229**, (B) **C219**, (C) **C249** or (D) **C250** alone (red curve), and pinhole defect filling with filler **III** (blue curve), measured under an irradiance of 100 mW cm^{-2}, simulated AM 1.5 sunlight.

References

S1   R. Li, J. Liu, N. Cai, M. Zhang and P. Wang, *J. Phys. Chem. B*, 2010, **114**, 4461.

S2   Y. Bai, J. Zhang, D. Zhou, Y. Wang, M. Zhang and P. Wang, *J. Am. Chem. Soc.*, 2011, **113**, 11442.

S3   M. Kašpar, H. Sverenyák, V. Hamplová, S. A. Pakhomov and M. Glogarová, *Mol. Cryst. Liq. Cryst.*, 1995, **260**, 241.

S4   R. Li, X. Lv, D. Shi, D. Zhou, Y. Cheng, G. Zhang and P. Wang, *J. Phys. Chem. C*, 2009, **113**, 7469.

S5   M. Xu, M. Zhang, M. Pastore, R. Li, F. De Angelis and P. Wang, *Chem. Sci.*, 2012, **3**, 976.

S6   W. Zeng, Y. Cao, Y. Bai, Y. Wang, Y. Shi, M. Zhang, F. Wang, C. Pan and P. Wang, *Chem. Mater.*, 2010, **22**, 1915.

S7   N. Cai, Y. Wang, M. Xu, Y. Fan, R. Li, M. Zhang and P. Wang, *Adv. Funct. Mater.*, 2013, **23**, 1846.

S8   P. Wang, S. M. Zakeeruddin, P. Comte, R. Charvet, R. Humphry-Baker and M. Grätzel, *J. Phys. Chem. B*, 2003, **107**, 14336.

S9   N. Cai, R. Li, Y. Wang, M. Zhang and P. Wang, *Energy Environ. Sci.*, 2013, **6**, 139.

S10   E. M. J. Johansson, M. Hedlund, H. Siegbahn and H. Rensmo, *J. Phys. Chem. B*, 2005, **109**, 22256.

S11   M. F. Hochella and A. H. Carim, *Surf. Sci.*, 1988, **197**, L260.

S12   P. J. Cumpson, *Surf. Interface Anal.*, 2001, **31**, 23.

S13   A. Nelson, *J. Appl. Cryst.*, 2006, **39**, 273.

S14   L. Luo, C.-F. Lo, C.-Y. Lin, I.-J. Chang and E. W.-G. Diau, *J. Phys. Chem. B*, 2006, **110**, 410.

S15   V. Shklover, Y. E. Ovchinnikov, L. S. Braginsky, S. M. Zakeeruddin and M. Grätzel, *Chem. Mater.*, 1998, **10**, 2533.